LBNL-43378

ERNEST ORLANDO LAWRENCE BERKELEY NATIONAL LABORATORY

Imaging Spectroscopic Analysis at the Advanced Light Source

A.A. MacDowell, T. Warwick, S. Anders, G.M. Lamble,
M.C. Martin, W.R. McKinney, and H.A. Padmore

Advanced Light Source Division

May 1999

REFERENCE COPY
Does Not
Circulate
Bldg. 50 Library - Ref.
Lawrence Berkeley National Laboratory
Copy 1
LBNL-43378

DISCLAIMER

This document was prepared as an account of work sponsored by the United States Government. While this document is believed to contain correct information, neither the United States Government nor any agency thereof, nor the Regents of the University of California, nor any of their employees, makes any warranty, express or implied, or assumes any legal responsibility for the accuracy, completeness, or usefulness of any information, apparatus, product, or process disclosed, or represents that its use would not infringe privately owned rights. Reference herein to any specific commercial product, process, or service by its trade name, trademark, manufacturer, or otherwise, does not necessarily constitute or imply its endorsement, recommendation, or favoring by the United States Government or any agency thereof, or the Regents of the University of California. The views and opinions of authors expressed herein do not necessarily state or reflect those of the United States Government or any agency thereof or the Regents of the University of California.

LBNL-43378

Imaging Spectroscopic Analysis at the Advanced Light Source

A.A. MacDowell, T. Warwick, S. Anders, G.M. Lamble,
M.C. Martin, W.R. McKinney, and H.A. Padmore

Advanced Light Source Division
Ernest Orlando Lawrence Berkeley National Laboratory
University of California
Berkeley, California 94720

May 1999

This work was supported in part by the Director, Office of Science, Office of Basic Energy Sciences, Materials Sciences Division, of the U.S. Department of Energy under Contract No. DE-AC03-76SF00098.

Imaging Spectroscopic Analysis at the Advanced Light Source

A.A. MacDowell, T. Warwick, S. Anders, G. M. Lamble, M. C. Martin, W. R. McKinney and H. A. Padmore

Lawrence Berkeley National Laboratory, Berkeley, CA94720, USA.

Introduction

One of the major advances at the high brightness third generation synchrotrons is the dramatic improvement of imaging capability. There is a large multi-disciplinary effort underway at the ALS to develop imaging X-ray, UV and Infra-red spectroscopic analysis on a spatial scale from a few microns to 10nm. These developments make use of light that varies in energy from 6meV to 15KeV. Imaging and spectroscopy are finding applications in surface science, bulk materials analysis, semiconductor structures, particulate contaminants, magnetic thin films, biology and environmental science.

This article is an overview and status report from the developers of some of these techniques at the ALS. The following table lists all the currently available microscopes at the ALS. This article will describe some of the microscopes and some of the early applications.

Table 1 .Spectromicroscopy Beamlines at the ALS

MICROSCOPY	BEAMLINE	ENERGY RANGE (eV)	RESOLUTION/FIELD
Infra Red FTIR	1.4.1	0.006 - 3.0	10um Probe
Full Field X-Ray Microscopy	6.1.2	50-950	43nm Full Field
Scanning X-Ray Microscopy	7.0.1	180 - 900	70nm Probe
Micro - XPS	7.0.1	200 - 800	150nm Probe
Micro - XPS	7.3.1.2	260 - 1500	1um Probe
Micro - XPS	12.0.1	95 & 130	100nm Probe
X-Ray Microprobe Broad Bandpass	10.3.1	8 & 12 KeV Multilayers	700nm probe
X-Ray microprobe Monochromatic	10.3.2	5 - 14 KeV	800nm Probe
Photoemission Electron Microscopy (PEEM)			
PEEM1	8.0.1	210 - 1200	200nm Full Field
PEEM2	7.3.1.1	260 - 1500	20nm Full Field

PEEM Microscopy at the ALS

Photoemission electron microscopy (PEEM) using X-rays is a full-field imaging technique based on the secondary electron emission caused by X-ray radiation and absorption. The secondary electrons are imaged by an electron optics column with a resolution given by the electron optics. By varying the incident X-ray wave length incrementally one is able to obtain local Near Edge X-ray Absorption Spectroscopy (NEXAFS) data with high spatial resolution.
There are two PEEM microscopes in operation at the ALS at the moment. The first one, called PRISM, is a two-lens system with a movable aperture in the backfocal plane of the objective lens [1]. The electron optics has a spatial resolution of 200 nm. The microscope is described in detail elsewhere [2]. It is located at beamline 8.0, an undulator beamline with an energy range of 200-1500 eV and a resolving power of E/DE=10000. The X-rays are focused on the sample by a Kirkpatrick-Baez pair of mirrors into a spot of 200um diameter.
A wide variety of materials and systems have been studied using this microscope including polymers, diamond-like carbon and diamond, various phases of titanium disilicide and of boron nitride, small particles, electron field emission materials, and ceramics (metal nitrides and oxides). In the following, a few examples will be given:

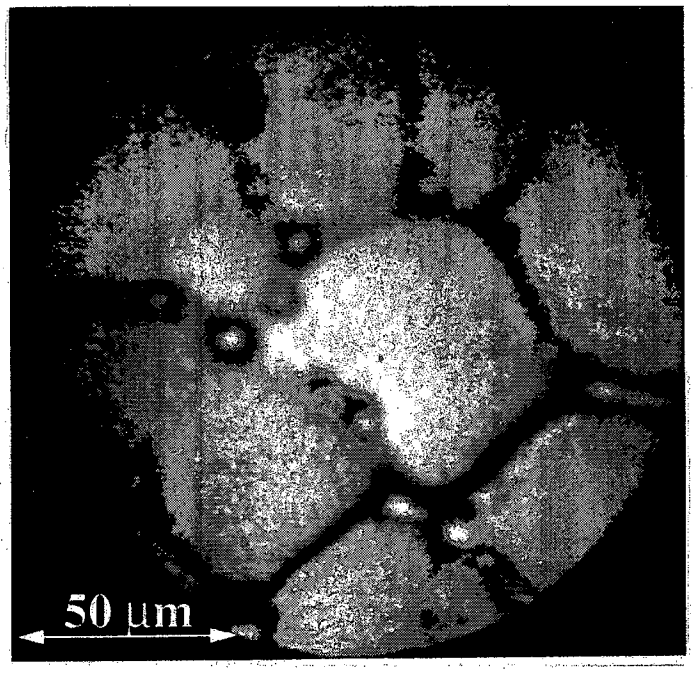

Figure 1. PEEM image of bilayer of PS and PBrS after 4 days of annealing at 180degC. Image was aquired at 286.3 eV. The contrast is due to topography since in the later phase of dewetting the surface is covered completely by PS.

Polymers are very suitable systems for X-ray microscopy studies because the K edges of the elements typically present in polymers (C, N, O, F, Br...) show very strong, sharp, and characteristic resonances for determining the chemical bonding states of the elements [3]. Polymers are used in many technological applications such as colloid paint systems, thin films for the alignment of liquid crystals in liquid crystal displays, lubricants on hard

disks, photoresist, to name only those applications we have studied so far. We have studied bilayer systems of polystyrene (PS) and brominated polystyrene (PBrS) consisting of a 30 nm thick PBrS layer on top of a 30 nm thick PS layer produced by spin casting [4]. The samples were annealed for various durations at 180degC and studied by scanning transmission electron microscopy (STXM) and PEEM. The formation of spines as a result of the dewetting process of the two polymers was observed with both methods. STXM was used to identify that the spines are composed of brominated polystyrene. The PEEM results showed that the dewetting of the PBrS starts in small areas exposing the PS underlayer, and in the later phase leads to a complete coverage of the surface with a thin PS film including the PBrS spines. Fig. 1 shows a PEEM image of a sample which was annealed for 4 days.

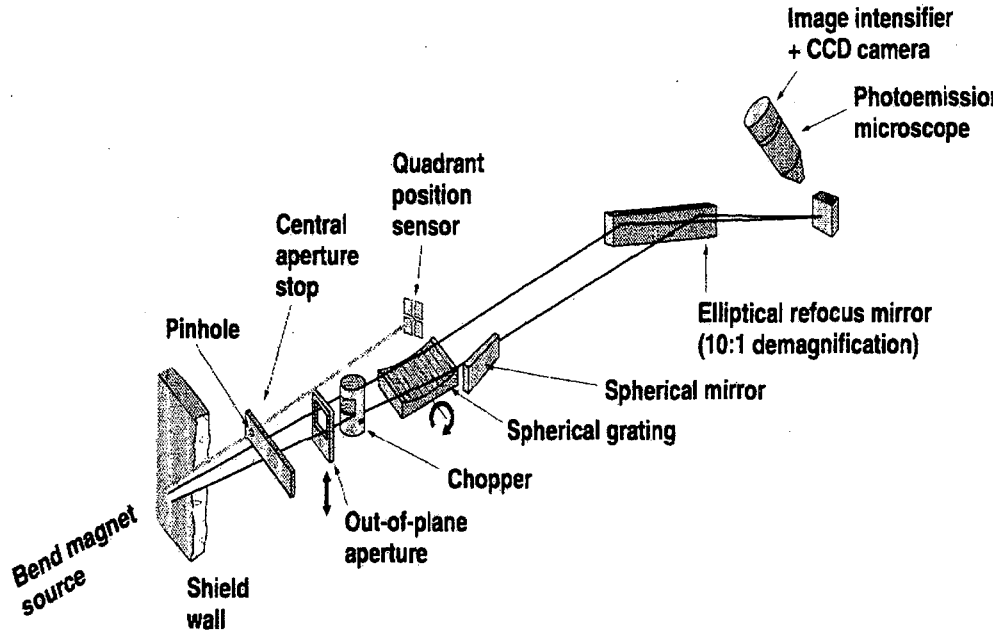

Figure 2 Schematic layout of beamline 7.3.1.1. at the ALS.

In another series of experiments the tribo-chemical behavior of lubricants on hard disks after wear and the transport of lubricants to the slider surface was studied [5]. It was found that the perfluoropolyether lubricant on the disk undergoes chemical changes during the wear. Fluorine is removed from the polymer, and oxidation in the form of carboxylic bonds takes place. Local NEXAFS spectra taken in wear tracks and on slider surfaces showed that this degraded lubricant is present in wear tracks, but it is also transferred to slider surfaces and accumulated in particular in scratches at the slider.

The new microscope PEEM2 is installed at the bending magnet beamline 7.3.1.1. which provides soft X-rays in the energy range from 250-1500 eV with a resolving power of E/dE=1800. Fig. 2 shows a schematic of the beamline. The X-rays are focused to a 30um spot on the sample. The beamline was designed specifically for XMCD experiments and is equipped with a mask and chopper to select above plane and below plane radiation (left and right circular polarized) and in plane radiation (linear polarized).

The microscope has been developed to study mainly magnetic materials using X-ray Magnetic Circular Dichroism (XMCD) at high resolution. The electron optics of the microscope consists of an electrostatic system of four lenses, a stigmator, and two

deflectors to correct for misalignment. The elements of the electron optics column are shown in Fig. 3. The operation voltage is 30 kV. In situ heating up to 1500degC and evaporation is possible. An automated sample transfer system allows fast sample exchange, and a sample preparation chamber is equipped with a sputter gun, a heater, and evaporators. The PEEM2 is currently in the commissioning phase. First images have been acquired, and elemental and magnetic contrast has been demonstrated. The calculated resolution limit of PEEM2 is 20-30 nm.

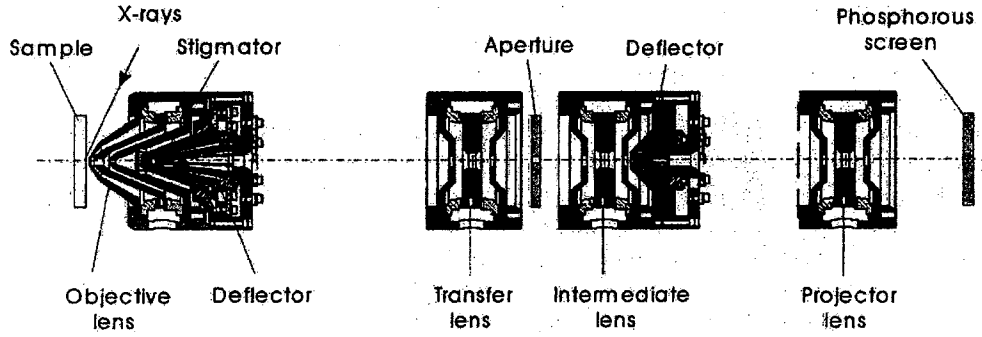

Figure 3 Schematic layout of PEEM2. Part of the lens design was adapted from an existing X-ray transmission microscope [5].

Scanning Zone Plate Microscopes for sub-micron NEXAFS and XPS

Two scanning zone plate microscopes have been developed for x-ray spectroscopic analysis of materials [7],[8]. These instruments operate in tandem at undulator beamline 7.0 at the ALS. A focused x-ray spot is rastered over the sample to make an image, then held on a feature of interest for spectral measurements. The count rates in these microscopes are about ten times higher than previously available. We are presently using zone-plate lenses with a central stop and 80nm outer zone width, and a corresponding diffraction limit to the spatial resolution of about 100nm. An order sorting aperture (OSA) is held in front of the sample and precisely positioned on the optical axis (+/-2 microns) to allow only the first order diffracted focus to reach the sample. The measured FWHM of the x-ray spot is 130nm.

The Scanning Transmission X-ray Microscope (STXM) provides imaging NEXAFS analysis of samples in transmission at atmospheric pressure. The transmission geometry is the most efficient use of photons for an absorption spectrum, well suited to radiation sensitive organic samples [9]. Measurements in transmission are bulk sensitive, so that surface contamination is not a concern, this allows the operation of the microscope at atmospheric pressure, in air or helium, with hydrated samples for problems in environmental science [10],[11]. Circularly polarized photons have been generated and used for imaging domains at the L edge in Fe, Ni and Co magnetic films [12]. We have measured 2 x 10^7 photons/second with a spectral width 1/3000 in the zone plate first order focus spot at 300eV, with the storage ring running at 1.5 GeV, 400mA. Figure 4. shows a case study illustrating the capability of STXM to perform polarization sensitive spectromicroscopy of organic polymers at the K edge of the three most important atomic species, C, N and O.

The Scanning Photo-Electron Microscope (SPEM) provides imaging XPS and NEXAFS analysis of sample surfaces in a UHV environment. Here the sample is

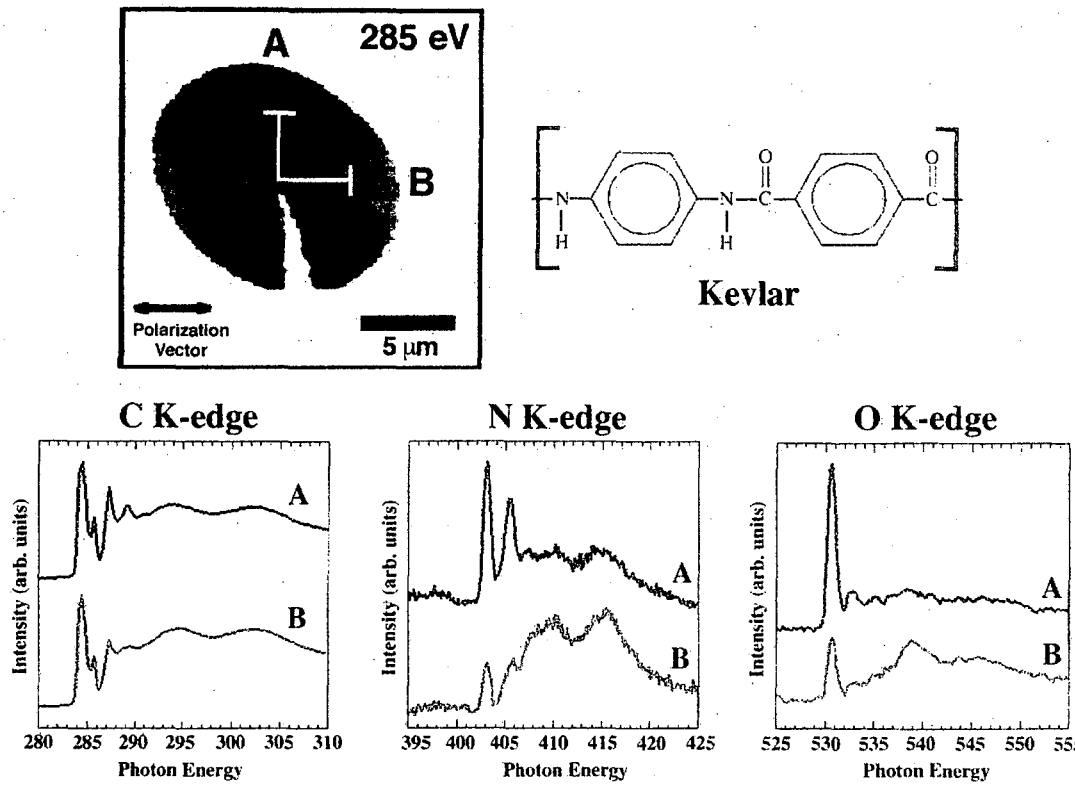

Figure 4. A sectioned Kevlar fiber measured in STXM (results courtesy of H. Ade and A. Garcia). Absorption spectra are measured at points A and B, showing the dependence on the angle between the photon polarization vector (horizontal) and the preferentially tangential orientation of the pi bonds of N and O. The polarization contrast reverses between the pi and sigma orbital peaks.

stationary during imaging and the zone plate is rastered in the illumination field to carry the focused spot across the sample surface. The illumination is of the order of 1mm diameter and the raster range is 80x80 microns. The electron spectrometer can view the entire range of the image area and collects photo-electrons at 60 degrees from the sample normal. The OSA is within 0.5mm of the sample surface, and the zone plate assembly is cut back on one side to allow a line of sight for the spectrometer. NEXAFS capability is included by means of a UHV flexure to carry the zone plate 0.5mm longitudinally to retain the focus condition as the photon energy changes. The OSA is fixed to the zone plate, with the focal length built in to the assembly. Different photon energies require different zone-plate/OSA combinations with different built-in focal lengths (e.g. 700eV for survey spectra including oxygen 1s photoelectrons, 270eV to 310eV for carbon K edge NEXAFS measurements). Five zone plates will be mounted together on a monolithic array with precisely parallel optical axes (to +/-1mrad), interchangeable under computer control. So far we have operated the microscope with three zone-plate/OSAs aligned in this way. SPEM allows us to perform quantitative XPS measurements of atomic concentration and core level chemical shifts over regions of the sample surface as small as the spatial resolution of the zone plate lens. The zone plate array can be lowered out of the beam and the sample surface can be observed with a magnifying video system, allowing visible fiducial marks on the sample to be used to position the region of interest

within the 100x100 micron range of the scan stage. XPS spectra are measured with typical photo-peak count-rates of 70,000 counts/second (Au 4f at 420eV photon energy).

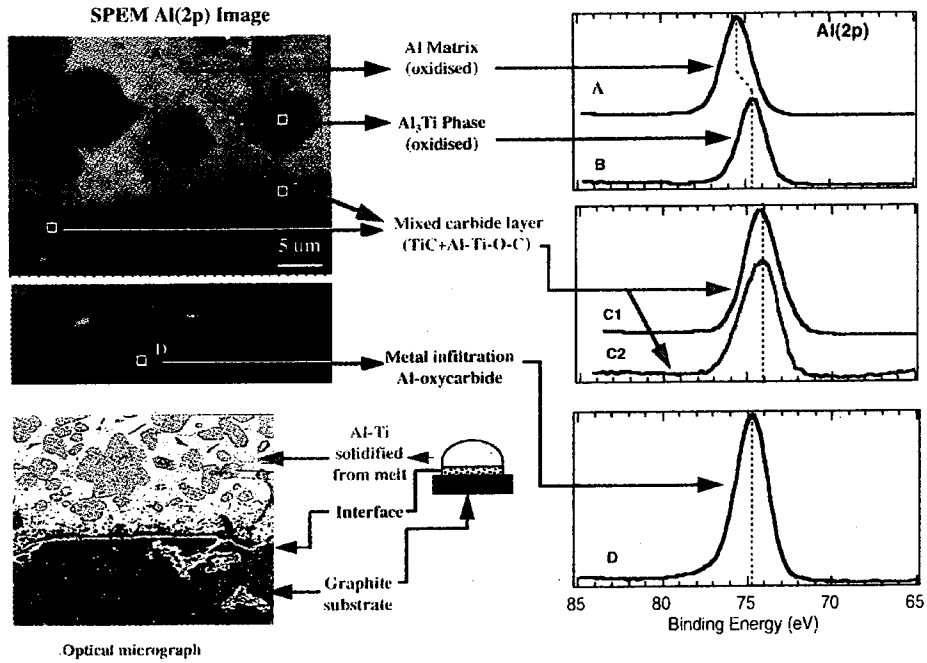

Figure 5. A SPEM case study in which an Al/Ti melt has been allowed to solidify on a graphite substrate (results courtesy S. Seal and N. Sobczak). The image of the polished section shows the aluminum metal, precipitates of Al_3Ti alloy and the graphite interface, with carbide formation. Different core level chemical shifts are observed from the Al, the Al_3Ti alloy and the carbide region. In this case sputtering has removed the adventitious carbon contamination but the surface is still oxidized.

X-Ray Micro-Diffraction

Kirkpatrick Baez (KB) mirrors have been developed in the hard x-ray energy range (2-15kev) [13]. This has allowed progress in the technique of x-ray micro-diffraction. The chosen problem area that defines the instrumental task appropriate to the capabilities of the ALS is the electromigation problem that affects the semiconductor industry. Electromigration is the physical movement of atoms in aluminum interconnect lines passing current at high electron density (typically in the range of 10^5 amp/cm^2). Significant material movement results in voids that consequently lead to breakage and circuit failure in the metal lines. This problem gets more severe as the line dimensions continue to shrink on integrated circuits. In spite of much effort in this field [14,15], electromigration is not understood in any depth or detail, but is strongly associated with the physical material properties (stress and strain) within the aluminum interconnect material. In addition these aluminum wires are buried in an insulating coating (usually SiO_2). X-rays are ideally suited to probe these buried metallic wires – the requirement being to establish the metallic grain orientation and strain (by measuring small changes in the d spacing) along the wire length. The aluminum grains are typically of size about a micron. The instrumental task is to carry out x-ray crystallography on micron sized samples.

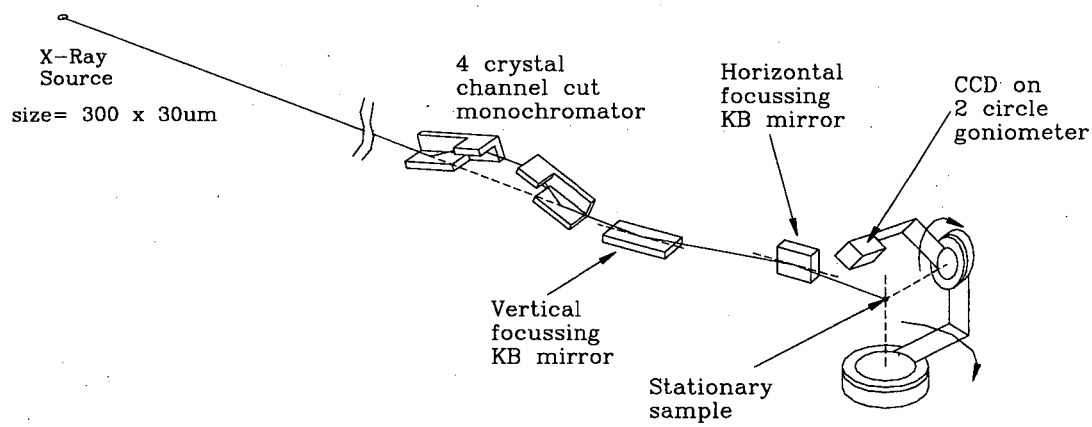

Figure 6 Schematic layout of the K-B mirrors and the four crystal channel cut monochromator.

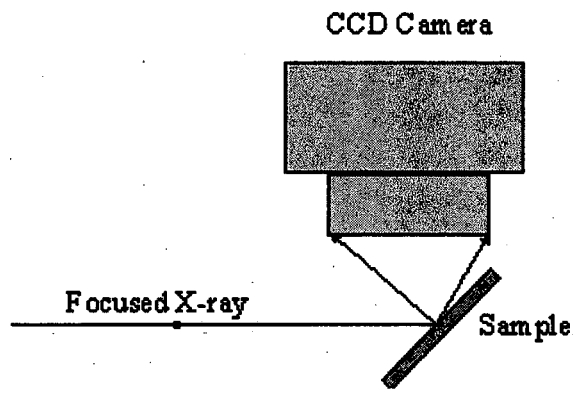

Figure 7. Schematic layout of the sample – CCD arrangement

Regular crystallography usually fixes the photon energy and scans the sample angle. If this were carried out with a micron sized sample and a micron sized x-ray probe, the sample and x-ray beam would rapidly become misalligned as the sphere of confusion of regular goniometers is typically tens of microns. We have adopted the alternative approach of fixing the sample position and scanning the photon energy. Figure 6 shows the schematic for the experimental setup. It consists of a 4 crystal monochromator (two channel cuts) at a distance of 31m from the bending magnet source followed by the KB mirrors which focus x-rays onto the sample. Spot sizes achieved to date are 0.8 microns FWHM. Diffracted x-rays from the sample are detected by a x-ray CCD. The monochromator crystals are mounted off axis which allows the ability to switch between white and monochromatic light whilst illuminating the same spot on the sample. The procedure for this micro-x-ray diffraction is first to find the sample – this is achieved by illuminating the grain of interest with white light and monitoring the Laue pattern with the sample to CCD geometry shown in Figure 7. A typical Laue image from an aluminum grain on a silicon (100) substrate is shown in Figure 8. The bright symmetric spots are those of the silicon substrate, but if one looks closely there are several weak asymmetric

spots from those of an aluminum grain misorientated with respect to the silicon substrate. Digitally subtracting the silicon spots results in the Laue pattern shown in figure 9, which can then be indexed. With the spots indexed the d spacing of the relevant planes can be measured by switching to monochromatic light and determining the photon energy of the individual Laue spots. d-spacings have been measured to 1 part in 10-3 which confirmed the indexation. To measure strain within the aluminum grain, d-spacing measurements some 10-100 times better are required. This work is underway with the delivery of a new custom built instrument capable of meeting the angular stability requirements.

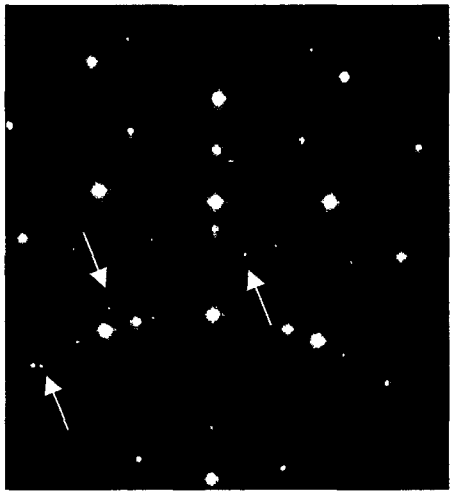

Figure 8 Laue pattern of a single grain in the aluminum interconnect line with the Laue pattern from the silicon substrate. Time for this exposure was 0.5 sec.

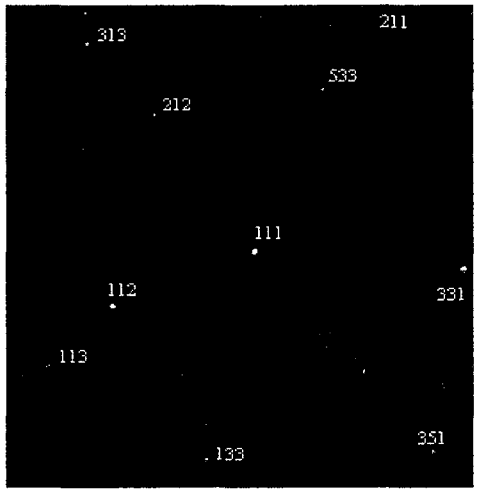

Figure 9 Laue pattern from just the aluminum grain after digitally subtracting the silicon Laue pattern.

Micro X-ray Absorption Spectroscopy and Micro X-ray Fluorescence for the Earth and Environmental Sciences

We have done some initial experiments using high spatial resolution determinations of elemental distribution and chemical specificity, on a test facility at the ALS using the intermediate X-ray energy range (2-15 keV) for the earth and environmental sciences in order to determine project feasibility. The equipment used is the same as used for micro diffraction (Fig.6) but with a SiLi fluorescence detector. The two techniques, X-ray Fluorescence Microscopy (XRFM) and Micro-X-ray Absorption Fine-structure Spectroscopy (XAFS), provide characterization probes on the micron scale [13], and thus the study of highly heterogeneous systems. These probes are ideally suited for the study of a variety of scientific problems in the earth and environmental sciences which have previously not been possible to measure or understand. In addition, the appropriate control of time and experimental conditions will provide mechanistic information and new insight into the interaction of such complex systems. Research areas which could directly benefit from this facility include: transport of nutrients and contaminants in plants and symbiotic systems; phytoremediation and phytostabilization mechanisms;

mobilization of nutrients or contaminants by colloids; mechanism of formation and function of biominerals in plants and animals; information about diagenesis, climate change and life forms by the investigation of the latter. Very little detail is known about many of the above systems. This is largely due to the lack of available tools to investigate the systems in their natural environment, using probes that are sufficiently small to investigate the changes on the scale with which they were occurring. We present some initial measurements made on various systems of interest.

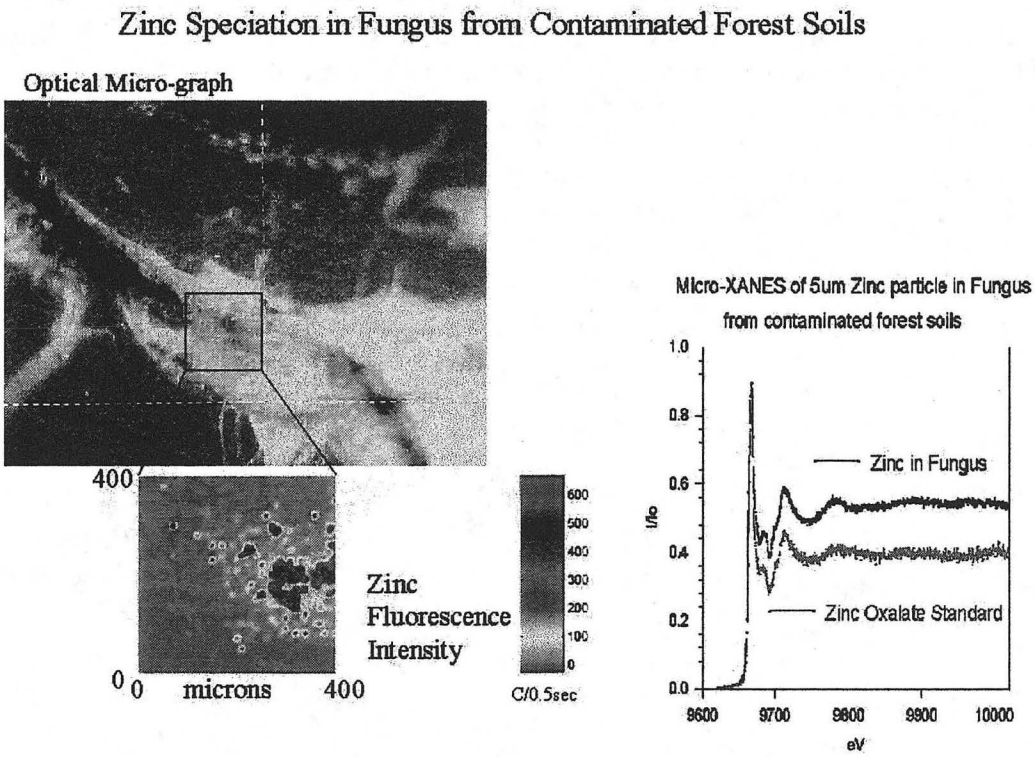

Figure 10. Zn-speciation in fungus from contaminated forest soils. A zinc elemental fluorescence map (lower left) was made from the 400x400 micron area of interest on the optical micrograph of the fungi in its natural state (top left). This map shows that the Zn is localized in very small regions of dimensions on only a few microns. Also included are a zinc XAFS spectrum taken from a 5 micron region of high Zn concentration along with a spectrum of a zinc oxalate standard.

The first measurements shown are from an ongoing study, in collaboration with researchers at the Norwegian University of Science and Technology [16], on the ability of particular fungi to hyperaccumulate certain contaminant metals. We are studying live fungi from the top organic layer of surface soils in the forest lands of southern Norway. These soils are substantially contaminated by a variety of heavy metals (Zn, Cu, Pb, Cd). It is known that the fungi take up and retain great quantities of the heavy metals but little is known of the precise forms in which they are retained nor of the mechanisms of uptake and conversion.

Figure 10 shows an optical micrograph of fungi in its natural state (top left). A 400 X 400 micron area of interest is marked on the image with the Zinc elemental fluorescence map from this area (lower left). This map shows that the Zn is localized in very small

regions of dimensions of only a few microns. Also included are a zinc XAFS spectrum taken from a 5 micron region of high Zn concentration along with a spectrum a zinc oxalate standard. The signal/noise is sufficiently good to scan some way into the Extended XAFS region, which indicates the potential for extracting structural parameters for this system. In this case a preliminary analysis of the short extended region is consistent with the observation by simple comparison with the very distinctive XAFS from the zinc oxalate standard, that there is a high likelihood that this species is Zinc oxalate. In addition, our conclusion supports that of recent work by Sarret et al. [17] which showed, using conventional XAFS, that for zinc sequestered by lichen (a symbiotic microorganism consisting of an algae and a fungi) under similar conditions of contaminant exposure, the dominant product is zinc oxalate.

This experiment demonstrates the capability of making a direct species determination on a very small spatial scale. The results suggest that zinc oxalate is an important intermediate in the retention or conversion of Zn by these fungi in their symbiotic relationship with the trees.

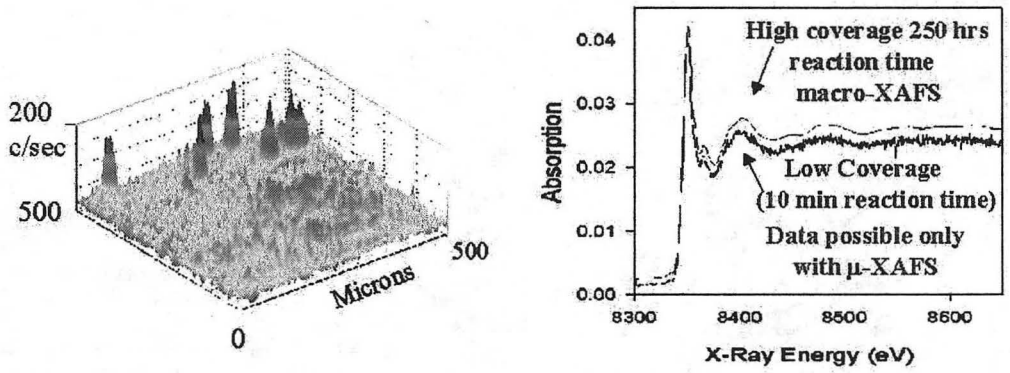

Figure 11. (Left) Map of Ni K edge fluorescence for a low coverage phase (10 min reaction time for interaction of clay surface with Ni ions) showing regions of local concentration of Ni. (Right) - Micro XAS data from initial studies of Ni reaction with clay (pyrophyllite) after short (10mins) reaction time and long (250 hours) reaction time.

We have made some preliminary measurements to the study of the kinetics of formation of mixed metal hydroxides on the surfaces of various clays. Recent XAFS measurements made at the NSLS in studies by Donald Sparks' group at the university of Delaware made an important contribution to the understanding of metal ion retention in the environment[18,19,20]. It was found that, under certain conditions of pH and concentration, nickel forms nickel-aluminum hydroxides on the surfaces of a number of clays. These hydroxides are quite resistant to dissolution and less soluble and thus severely reduce the mobility of Ni in the environment. It is thought that the same behavior will apply to a large number of other metal contaminants; the main criteria being that the ionic radius should be close to that of the aluminum cations.

In the Ni study XAFS spectra were taken at various reaction times of the clay surface with the Ni ions. Despite the clear conclusion that mixed metal hydroxides were forming, it was unfortunately not possible to interpret XAFS data from the low coverages (below

15 minutes reaction time) since the macroscopic concentration was too low and the XAFS data was too noisy.

XRFM measurements of one of the low coverage structures were made at the ALS. These are shown in figure 11. It can be seen that some form of Ni aggregation or precipitation is already forming at these short reaction times. It was thus possible to make microXAFS measurements on these precipitates, which appeared to be a few microns in size. These data are shown in figure 15B along with data taken using the conventional technique of the longest reaction time (250 hours). These initial data indicate that the precipitates formed at these low coverages are of the same type as those formed at the higher coverages. This suggests that the mixed-metal "binding" of contaminants occurs close to the onset of adsorption which, in itself, has important implications for metal transport in the environment. More extensive studies are planned [21] in order to check the reproducibility of these initial results. This particular example shows how, in the case where there is aggregation and thus local concentration on the micron scale, how microXAFS can be more sensitive than the macroscopic technique and why the parameter describing absorber 'dispersion' is more meaningful than the macroscopic value of the concentration.

High Spatial Resolution FTIR Spectromicroscopy

Synchrotron-based infrared (IR) beamlines provide considerable brightness advantages over conventional IR sources [22]. This brightness advantage manifests itself most beneficially when measuring very small samples. In the commissioning of the first IR beamline at the ALS, beamline 1.4.3, we have experimentally measured the small spot-size obtained by our IR microscopy system when using the synchrotron beam as the source and we compare it to the internal Globar source. We demonstrate the resolution-limited focus and the corresponding factor of ~100 improvement over conventional sources in measured signal through very small apertures.

Synchrotron light from the 1.4 bending magnet at the ALS is collimated via a series of aluminum-coated mirrors [23], and is then distributed to one of three end-stations, as schematically drawn in Figure 12. Beamline 1.4.3 inputs the light into a Nicolet Magna 760 purged FTIR spectrometer. The modulated light then passes through a Nic-Plan all-reflecting IR microscope and onto a sample, allowing transmission or reflection measurements throughout the mid-infrared region.

To determine the spot-size at the focus of the IR-microscope, the transmission through a 10 micron aperture was measured as a function of aperture position on the computer-controlled sample stage. This stage has 1 micron spatial resolution, and the FTIR software obtains a spectral map of the transmitted light as a function of x and y position of the stage. No other beam-defining apertures were used. The resultant map of integrated IR intensity versus pin hole position is shown in Figure 13. Cuts of the data along the x- and y-directions result in Gaussian line shapes with widths of 10mm in x and 8mm in y. This spot size is becoming diffraction-limited for the low-energy end of our detection capabilities (1000cm-1 = 10mm wavelength).

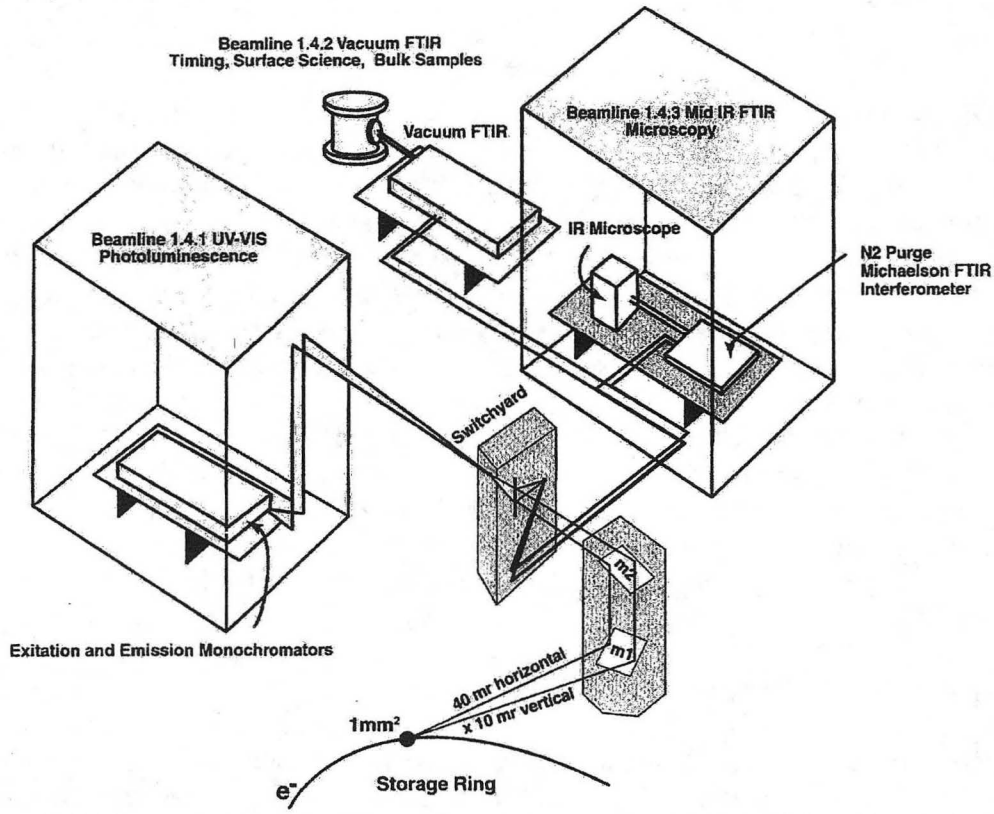

Figure 12 Schematic layout of beamlines 1.4.x at the ALS. 10 by 40 milliradians of synchrotron light from the 1.4 bending magnet port is collected and then collimated in the switchyard. The light is then directed to one of three end-stations which perform UV photoluminescence, vacuum FTIR, and IR spectromicroscopy, respectively.

When the above synchrotron measurements are compared to analogous measurements made with a conventional Globar IR source, the brightness advantages of the synchrotron become readily apparent. The Globar has a significantly broader peak profile of around 100mm in width simply due to the large source size of this glowing filament source making a better focus impossible. Therefore, while the overall flux from the Globar and the synchrotron sources is comparable, the synchrotron light can be focused onto a 10mm spot. To achieve a similar spot size using the conventional Globar source, one must simply mask the Globar source discarding a large factor of signal intensity. We have measured improvements of several hundred in intensity transmitted through small pin-holes for the synchrotron source compared to the Globar.

Experimental systems where the sample size is quite small, or where features on a sample are on the few micron size scale, will gain significantly by using ALS Beamline 1.4.3. A few examples include observing bacteria ingesting specific chemicals in real time, localization of adsorbates on environmental surfaces, particulate contamination on semiconductors, polymer laminates and composites, analytical forensic studies of small samples, and measuring materials at high pressure in diamond anvil cells. In summary, synchrotron IR spectromicroscopy enables a host of new scientific pursuits where spectral features can be mapped at the few micron spatial scale.

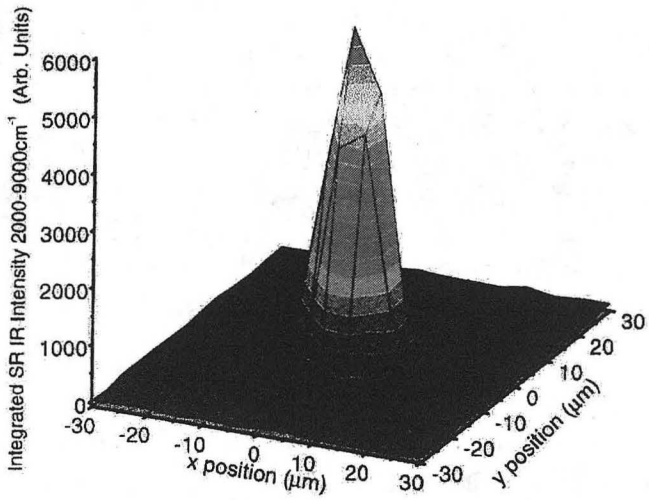

Figure 13. Integrated IR signal intensity from 2000 - 9000cm-1 through a 10mm pin hole being rastered on the IR-microscope stage. There are no other apertures in the optical path. This plot demonstrates the small spot size achieved using the synchrotron IR beam

Acknowledgements

This work was supported in part by the Director, Office of Basic Energy Sciences, Materials Sciences Division of the US Department of Energy, under Contract no. DE-AC03-76SF00098

References

[1] PRISM was built by B. Tonner and G. Castro, PEEM2 by S. Anders, M. Scheinfein, H. A. Padmore and J. Stöhr.

[2] B. P. Tonner, D. Dunham, T. Droubay, and M. Pauli, J. Electron Spectrosc. Relat. Phenom. 84 (1997) 211.

[3] J. Stöhr, NEXAFS Spectroscopy, Springer Verlag, New York, 1992.

[4] These experiments were performed by S. Anders and Th. Stammler (ALS), H. Ade (North Carolina State University), D. Slep (Hilord Chemical Corp.), J. Sokolov and M. Rafailovich (SUNY@Stony Brook), J. Stöhr (IBM), and C. Heske (ALS)

[5] S. Anders, Th. Stammler, C. S. Bhatia, J. Stöhr, W. Fong, C.-Y. Chen, and D. B. Bogy, Materials Research Society Spring Meeting, San Francisco 1998, to be published.

[6] R. N. Watts, S. Liang, Z. H. Levine, T. B. Lucatorto, F. Polack, aand M. R. Scheinfein, Rev. Sci. Instrum. 68 (1997) 3464.

[7] This program originated with a proposal from B. Tonner, Univ. Wisconsin et. al. with continuing development by the ALS.

[8] T.Warwick, H.Ade, S.Cerasari, J.Denlinger, K.Franck, A.Garcia, S.Hayakawa, A.Hitchcock, J.Kikuma, J.Kortright, G.Meigs, M.Moronne, S.Myneni, E.Rightor, E.Rotenberg, S.Seal, H-J.Shin, R.Steele. T.Tyliszczak and B.Tonner
J. Synchrotron Rad. 5 (1998) to be published

[9] E.G.Rightor, A.P.Hitchcock, H.Ade, R.D.Leapman, S.G.Urquhart, A.P.Smith, G.Mitchell, D.Fischer, H.J.Shin and T.Warwick

J. Phys. Chem. B 101(1997)1950
[10] S. C. B. Myneni, J. T. Brown, W. Meyer-Ilse, G. A. Martinez, A. Garcia and A. Warwick Abstracts of the AGU National Meeting, San Francisco, 1997
[11] T. Grundl, S. Cerasari, A. Garcia, T. Warwick, H. Ade and B.P Tonner Compendium of User Abstracts and Technical Reports 1993-1996, LBNL-39981 (1997)
[12] J.Kortright, S.K.Kim, T.Warwick and N.V.Smith. Appl. Phys. Lett. 71(1997) 1446
[13]A.A.MacDowell, R.Celestre, C.H.Chang, K.Franck, M.R.Howells, S.Locklin, H.A.Padmore, J.R.Patel, and R.Sandler, *SPIE Proceedings* 3152, 126-135 (1998).
[14] T.Marieb, P.Flinn, J.C.Bravman, D.Gardner, and et al. *J. App Phys.* 78, 1026-1032 (1995).
[15] P.C.Wang, G.S.Cargill, and I.C.Noyan, *MRS Proceedings* 375, 247-252 (1995).
[16] D.Nicholson, A. Moen, B. Berthelsen, G.M.Lamble, A.A.MacDowell, R.S.Celestre, H.A.Padmore, ALS Highlights 1997. (ii) G.M. Lamble, D.G. Nicholson, A. Moen and B. Bethelsen, submitted to XAFS X, Chicago, Il, Aug 1998.
[17]"Mechanisms of Lichen resistance to metallic Pollution: An in-situ EXAFS Study". G.Sarret, A.Manceau, D.Cuny, C.Van Haluwyn, M.Imbenotte, S.Derulle, J-L Hazemann, Fourth Int. Conf. Biogeochemistry of Trace Elements. June 23-28, (1997), U.C.Berkeley. (ii) Géraldine Sarret, PhD these, Observatoire De Grenoble et Laboratoire de Geophysique Interne et Tectonophysique (1998).
[18] Spectroscopic Evidence for the Formation of Mixed-Cation Hydroxide Phases Upon H.A.Padmore, J.R.Patel and R.Sandler, " Progress towards sub-micron x-ray imaging Metal Sorption on Clays and Aluminum Oxides, André M. Scheidegger, Geraldine M. Lamble and Donald L. Sparks, Journal of Colloid and Interface Science **186**, 118-128 (1997)
[19]The Kinetics of Nickel Sorption on Pyrophyllite as Monitored by X-Ray Absorption Fine Structure (XAFS) Spectroscopy, André M. Scheidegger, Geraldine M. Lamble and Donald L. Sparks, J. De Physique IV France **7 c2** 773-775, 1997.
[20]The Kinetics of Mixed Ni-Al Hydroxide Formation on Clay and Aluminum Oxide Minerals: A Time-Resolved XAFS Study, André M. Scheidegger, Daniel G. Strawn, Geraldine M. Lamble and Donald L. Sparks, Geochimica et Cosmochimica Acta (accepted).
[21]Andreas Scheinost, Robert Gale Ford, Geraldine M. Lamble and Donald L. Sparks (In progress).
[22]Hirschmugl, C.J., PhD Thesis Yale University, 1994.
[23] W.R. McKinney, C.J. Hirschmugl, H.A. Padmore, T. Lauritzen, N. Andresen, G. Andronaco, R. Patton, and M. Fong, Proceedings of the SPIE, "Accelerator-Based Infrared Sources and Applications" Volume 3153, pp 59-67.

Ernest Orlando Lawrence Berkeley National Laboratory
One Cyclotron Road | Berkeley, California 94720

Prepared for the U.S. Department of Energy under Contract No. DE-AC03-76SF00098